Title
Imaging and quantifying transverse flow velocity with the Doppler bandwidth in a phase-resolved functional optical coherence tomography.

Journal
Optics letters, 27(6)

ISSN
0146-9592

Authors
Ren, Hongwu
Brecke, Kjell Morten
Ding, Zhihua
et al.

Publication Date
2002-03-01

DOI
10.1364/ol.27.000409

Imaging and quantifying transverse flow velocity with the Doppler bandwidth in a phase-resolved functional optical coherence tomography

Hongwu Ren, Kjell Morten Brecke, Zhihua Ding, Yonghua Zhao, J. Stuart Nelson, and Zhongping Chen

The Center for Biomedical Engineering and Beckman Laser Institute, University of California, Irvine, Irvine, California 92612

Received October 25, 2001

The Doppler bandwidth extracted from the standard deviation of the frequency shift in phase-resolved functional optical coherence tomography (F-OCT) was used to image the velocity component that is transverse to the optical probing beam. It was found that above a certain threshold level the Doppler bandwidth is a linear function of flow velocity and that the effective numerical aperture of the optical objective in the sample arm determines the slope of this dependence. The Doppler bandwidth permits accurate measurement of flow velocity without the need for precise determination of flow direction when the Doppler flow angle is within $\pm 15^\circ$ perpendicular to the probing beam. Such an approach extends the dynamic range of flow velocity measurements obtained with the phase-resolved F-OCT. © 2002 Optical Society of America

OCIS codes: 170.4500, 110.4500.

Optical Doppler tomography (ODT) combines Doppler velocimetry with optical coherence tomography[1] (OCT) for noninvasive localization and measurement of particle-flow velocity in highly scattering media with micrometer-scale spatial resolution.[2–6] ODT uses a low-coherence source and an optical interferometer to obtain high-spatial-resolution gating of photons at a user-specified depth in biological tissues or other turbid media. In combination with a high-speed scanning device such as a rapid-scanning optical delay line,[7,8] ODT permits ranging of microstructure and particle motion. Several ODT algorithms and hardware schemes have been developed to detect the Doppler frequency shift produced by moving particles. The most straightforward method for determining frequency shift is to use a short-time fast Fourier transformation.[2–4] However, the sensitivity of this method depends mainly on the fast Fourier transform time window, which limits axial scanning speed and spatial resolution when one is measuring slow-moving blood flow in small vessels. A phase-resolved technique[5,6] can decouple the Doppler sensitivity and spatial resolution while maintaining high axial scanning speed. A previous Letter[6] on phase-resolved functional OCT (F-OCT) demonstrated how one can use the standard deviation of the Doppler spectrum to locate the microvasculature. In this Letter we demonstrate that one can use the spectral bandwidth of the Doppler frequency shift (Doppler bandwidth) to provide quantitative information on flow velocity.

There are a number of sources, including velocity gradient, turbulence, Brownian motion, speckle, and probe-beam geometry, that contribute to broadening of the Doppler spectrum. When flow velocity is low, Brownian motion dominates the broadening of the Doppler spectrum. When velocity is high, probe-beam geometry dominates. The contribution of focusing-beam geometry can be derived from geometrical optics, as shown in Fig. 1. When the Doppler angle is larger than $\tan^{-1}(2w/l_c)$, where w is the waist radius of the Gaussian optical beam at the focal point and l_c is the source coherence length, the Doppler bandwidth is determined by the difference between the two extreme average Doppler frequency shifts f_a and f_b, caused by the two optical rays at the two outer boundaries of the probe beam:

$$B_d = f_a - f_b = \frac{4V}{\lambda} \sin\phi \sin\theta = \frac{4V \sin\theta \, \mathrm{NA}_{\mathrm{eff}}}{\lambda}, \tag{1}$$

where B_d is the Doppler bandwidth defined by geometrical optics, V is the flow velocity, ϕ is the optical aperture angle, θ is the Doppler angle, λ is the center wavelength of the light source, and $\mathrm{NA}_{\mathrm{eff}}$ is the effective numerical aperture. For a Gaussian optical beam, the Doppler bandwidth $B_{1/e}$ (full width at $1/e$ of maximum spectrum amplitude) is the inverse of the transit time spent by particles passing through the focus zone:

$$B_{1/e} = (\pi/8) B_d . \tag{2}$$

Considering the relationship between standard deviation σ and the Doppler bandwidth for a Gaussian optical beam,

$$B_{1/e} = 4\sigma , \tag{3}$$

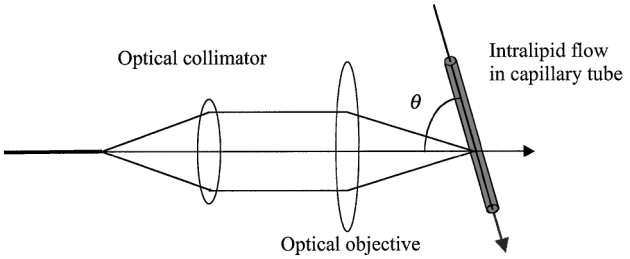

Fig. 1. Probe-beam geometry in the sample arm of the interferometer; θ, Doppler angle.

0146-9592/02/060409-03$15.00/0

we can write the relationship between the standard deviation and NA_{eff} as

$$\sigma = \frac{\pi V \sin\theta \, NA_{eff}}{8\lambda} . \quad (4)$$

If contributions from Brownian motion and other sources that are independent of the macroscopic flow velocity are included, Eq. (4) can be modified as

$$\sigma = \frac{\pi V \sin\theta \, NA_{eff}}{8\lambda} + b , \quad (5)$$

where b accounts for spectrum broadening owing to Brownian motion, velocity gradient, turbulence, and the speckle nature of the F-OCT signal.

Equation (5) indicates that, above a threshold value, the Doppler bandwidth is a linear function of flow velocity. The effective numerical aperture NA_{eff} of the optical objective in the sample arm determines the slope of this linear dependence. When the flow velocity is much higher than this threshold value and NA_{eff} is known, the linear dependence of the Doppler bandwidth permits accurate measurement of the flow velocity that is transverse to the optical axis of the probe beam.

The experimental system used for Doppler bandwidth measurements was described previously.[5,6] The interferometer uses a low-coherence amplified spontaneous emission broadband source whose output power, center wavelength, and bandwidth are 5 mW, 1300 nm, and 65 nm, respectively. The source light is coupled into the interferometer and split into reference and sample arms by a 3-dB 2×2 coupler. A rapid-scanning optical delay line in a group-delay scanning mode is used for A-line scanning at 500 Hz. An electro-optical phase modulator is used in the reference arm to generate a 500-kHz carrier frequency. In the sample arm shown in Fig. 1, interchangeable optical collimator and optical objective (20×; numerical aperture, 0.35) are used to focus the beam at the center of a capillary tube with an inner diameter of 900 μm for M-mode imaging. A 0.1% Intralipid solution composed of particles of 0.356-μm diameter is used as the turbid liquid medium. A syringe pump driven by a high-resolution translation stage controls the flow of the Intralipid solution through the capillary tube. In the detection arm of the interferometer, the signal from the photodetector is amplified with a bandpass preamplifier and then sent to a 12-bit analog-to-digital converter and a data-acquisition board sampling at 5 MHz. The number of data points for each A-line data acquisition is 4096.

The dependence of the Doppler bandwidth of the Intralipid flow at the center of the capillary tube on numerical aperture NA_{eff}, Doppler flow angle θ, and flow velocity V was measured. The standard deviation profiles for Intralipid flow in the capillary tube for three different flow velocities are shown in Fig. 2 ($NA_{eff} = 0.09$ and $\theta = 77°$). The background b value for these curves is approximately 72 Hz. The measured and predicted standard deviations of the Doppler spectrum as a function of flow velocity are shown in Fig. 3 ($NA_{eff} = 0.09$ and $\theta = 77°$). We extracted the data from the center of the tube that corresponds to the top of the parabolic flow profile to study the relationship between Doppler bandwidth and velocity. The standard deviation of the Doppler spectrum from experimental measurements (open circles for NA_{eff} 0.09 and open triangles for NA_{eff} 0.05) and the theoretical predications from Eq. (5) (solid curves) are in good agreement for flow velocities larger than 300 μm/s. At low flow velocities, the standard deviation is constant because the Doppler bandwidth is dominated by broadening caused by Brownian motion, which is independent of flow velocity. For velocities higher than 300 μm/s, the Doppler bandwidth is dominated by broadening that is due to the probe beam's geometry. The Doppler bandwidth is a linear function of velocity, with the slope determined by NA_{eff}. The measured and predicated standard deviation values are shown as a function of Doppler angles when the flow velocity is 698 μm/s in Fig. 4. The results indicate that the Doppler bandwidth is insensitive to variation in the Doppler angles when the angle is within ±15° perpendicular to the probe beam.

Phase-resolved F-OCT increases the sensitivity of flow velocity detection by more than 2 orders of

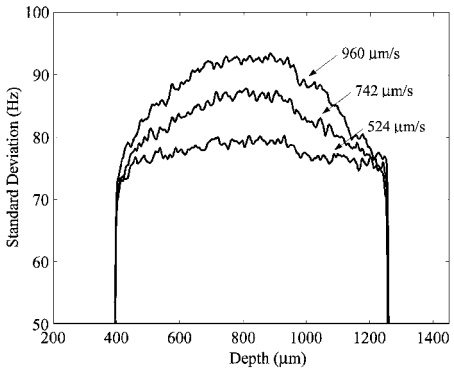

Fig. 2. Standard deviation flow profiles at the center of a glass capillary tube with an inner diameter of 900 μm. Background b for these curves is approximately 72 Hz.

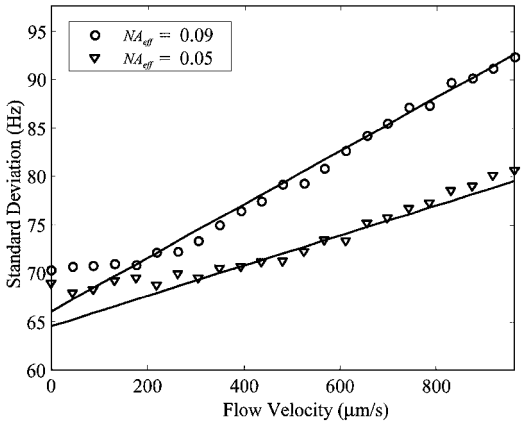

Fig. 3. Standard deviation NA as a function of flow velocity for two numerical apertures at a Doppler angle of 77°. Solid curves, theoretical curves calculated with Eq. (5).

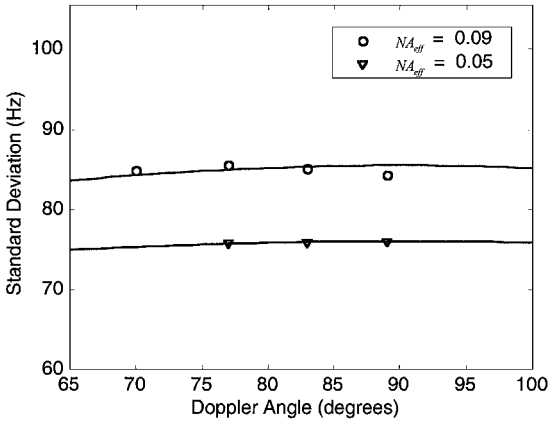

Fig. 4. Standard deviation NA as a function of Doppler flow angle for two values of NA_{eff} when the flow velocity is 698 μm/s. Background b when NA_{eff} is 0.09 or 0.05 is 65.6 or 64.8 Hz, respectively.

magnitude while at the same time increasing the imaging frame rate. However, F-OCT has a limited dynamic range because of an aliasing phenomenon caused by 2π ambiguity in the arctangent function. The maximum unambiguous velocity $V_{\max}{}^{f_d}$ detected by F-OCT for a given A-line scan frequency f_s is given by

$$V_{\max}{}^{f_d} = \frac{\lambda}{4 \cos \theta} f_s . \tag{6}$$

The flow velocity measured by the Doppler bandwidth has a larger dynamic range than that measured by direct Doppler shift. The standard deviation is similarly limited by the aliasing phenomenon described by $\sigma \leq f_s$. However, because σ is only a small fraction of the average Doppler frequency shift encountered in most clinical situations, the unambiguous detection range of velocities for the Doppler bandwidth method can be as much as 10–20 times larger than that of the corresponding phase-resolved method with the Doppler angle in the range of 70°–120°. Such an increase in dynamic range was confirmed by our experiments. As shown in Fig. 3, there is no aliasing phenomenon even though the velocity has reached 960 μm/s, which is much higher than the measurable velocity range.

In summary, Doppler bandwidth can be used to measure flow velocity that is transverse to the probing beam. Above a threshold value, the Doppler bandwidth is linearly dependent on flow velocity, and the effective numerical aperture of the optical objective determines the slope of this dependence. When the Doppler flow angle is within ±15° perpendicular to the probe beam, the average Doppler frequency shift is highly sensitive to angle position, but the Doppler bandwidth is insensitive to flow direction. Therefore the linear dependence of flow velocity on Doppler bandwidth permits accurate measurement of the flow velocity without precise determination of flow direction.

This study was supported by research grants from the National Institutes of Health (HL-64218, RR-01192, and GM-58785), the National Science Foundation (BES-86924), and the Defense Advanced Research Projects Agency BioFlips Program (N66001-C-8014). Institutional support from the U.S. Air Force Office by Scientific Research (F49620-00-1-0371), the U.S. Department of Energy (DE-FG03-91ER61227), and the Beckman Laser Institute Endowment is gratefully acknowledged. Z. Chen's e-mail address is zchen@bli.uci.edu.

References

1. D. Huang, E. A. Swanson, C. P. Lin, J. S. Schuman, W. G. Stinson, W. Chang, M. R. Hee, T. Flotte, K. Gregory, C. A. Puliafito, and J. G. Fujimoto, Science **254,** 1178 (1991).
2. Z. Chen, T. E. Milner, D. Dave, and J. S. Nelson, Opt. Lett. **22,** 64 (1997).
3. Z. Chen, T. E. Milner, S. Srinivas, X. Wang, A. Malekafzali, M. J. C. van Gemert, and J. S. Nelson, Opt. Lett. **22,** 1119 (1997).
4. M. D. Kulkarni, T. G. van Leeuwen, S. Yazdanfar, and J. A. Izatt, Opt. Lett. **23,** 1057 (1998).
5. Y. Zhao, Z. Chen, C. Saxer, S. Xiang, J. F. de Boer, and J. S. Nelson, Opt. Lett. **25,** 114 (2000).
6. Y. Zhao, Z. Chen, C. Saxer, Q. Shen, S. Xiang, J. F. de Boer, and J. S. Nelson, Opt. Lett. **25,** 1358 (2000).
7. G. J. Tearney, B. E. Bouma, and J. G. Fujimoto, Opt. Lett. **22,** 1811 (1997).
8. A. M. Rollins, M. D. Kulkarni, S. Yazdanfar, R. Ung-arunyawee, and J. A. Izatt, Opt. Express **3,** 219 (1998), http://www.opticsexpress.org.